

# The ultrastructural and morphological characteristics of the anterior cruciate ligament of the pig: a study using 7.0-Tesla diffusion tensor imaging

Journal of International Medical Research

2022, Vol. 50(11) 1–7

© The Author(s) 2022

Article reuse guidelines:

[sagepub.com/journals-permissions](https://sagepub.com/journals-permissions)

DOI: 10.1177/03000605221121954

[journals.sagepub.com/home/imr](https://journals.sagepub.com/home/imr)



Tian You<sup>1</sup> , Fujia Jiao<sup>2,\*</sup>, Wentao Zhang<sup>1</sup>,  
Qingjun Yang<sup>3</sup>, Wenqian Lu<sup>4</sup> and Yong Luo<sup>5</sup>

## Abstract

**Objective:** Diffusion tensor imaging research on the anterior cruciate ligament (ACL) is limited, and no study has revealed the ACL fibrous microstructure by 7.0-Tesla magnetic resonance imaging. Therefore, we used magnetic resonance imaging to assess the ACL.

**Methods:** Eight porcine ACLs were investigated by diffusion tensor imaging. Imaging was performed with a 7.0-Tesla scanner using a diffusion-weighted two-dimensional spin-echo echo-planar imaging pulse sequence optimised for muscle. The diffusion tensor eigenparameters, fractional anisotropy (FA), and apparent diffusion coefficient (ADC) were used for bones and muscles. Three-dimensional projection maps of the principal eigenvectors were plotted to visualise the microstructure.

**Results:** The mean FA and ADC for the ACL were  $0.27 \pm 0.079$  and  $0.0012 \pm 0.0005$ , respectively. There were no significant differences between the values in the proximal and distal portions. However, the ADC was smaller in the centre than on the sides ( $0.0015 \pm 0.0007$ ), and the mean FA was larger in the centre than on the sides ( $0.42 \pm 0.23$ ). The ACL fibres were parallel on the proximal and distal sides but interweaved in the centre.

**Conclusions:** These findings may be beneficial for artificial ligaments.

<sup>1</sup>Sports Medicine Department, Peking University Shenzhen Hospital, Shenzhen, China

<sup>2</sup>School of Exercise and Health, Shanghai University of Sport, Shanghai, China

<sup>3</sup>Clinical Medical College, Weifang Medical University, Weifang, China

<sup>4</sup>Health Science Center, Shenzhen University, Shenzhen, China

<sup>5</sup>Department of Clinical Medicine, Shantou University Medical College, Shantou, China

\*Fujia Jiao is the co-first author.

## Corresponding author:

Wentao Zhang, Sports Medicine Department, Peking University Shenzhen Hospital, 1120 Lianhua Road, Futian District, Shenzhen, Guangdong Province 518036, China.  
Email: [zhangwtshenzhen@163.com](mailto:zhangwtshenzhen@163.com)



## Keywords

Anterior cruciate ligament, diffusion tensor imaging, fibrous microstructure, eigenparameter, fractional anisotropy, apparent diffusion coefficient

Date received: 30 January 2022; accepted: 1 August 2022

## Introduction

Diffusion tensor imaging (DTI) is the outcome of advancements in diffusion-weighted imaging, in which the diffusion of water molecules is used to evaluate the structure and physiological state of biological tissues. The distances that the molecules diffuse in one direction along the space are equal (isotropic) or unequal (anisotropy). Magnetic resonance imaging (MRI) is used to track hydrogen atoms in water molecules, and DTI maps the direction of movement of water molecules.<sup>1,2</sup>

Injuries involving the anterior cruciate ligament (ACL) are among the most common forms of knee injuries, and these injuries have a major effect on the stability and flexibility of the knee joint.<sup>3</sup> In addition to manual examinations, MRI is used in patients with ACL injuries to assess the ligaments and can effectively show damage in up to 90% of cases.<sup>4</sup> MRI can also indicate the state of water molecules in living tissues without affecting the diffusion process,<sup>5</sup> making it the most ideal method for detecting the diffusion of water molecules in living tissues. In these examinations, a higher magnetic field intensity is associated with a clearer image.<sup>6</sup>

DTI is currently the only non-invasive method that can facilitate effective observation and tracking of white-matter fibre bundles. It is widely used in the brain, especially for observation and tracking of the white matter tract, brain development, brain cognitive function, pathological changes in brain diseases, preoperative planning and postoperative evaluation of patients undergoing brain surgery, and myocardial

function.<sup>5,7,8</sup> However, the literature regarding the use of this technique to study human skeletal muscle injuries and tendons is limited.<sup>9–11</sup> Chen et al.<sup>12</sup> and Delin et al.<sup>13</sup> reported that diffusion-weighted imaging can improve the specificity of conventional MRI for assessment of ACL tears and can be used for quantitative analysis, allowing evaluation of the complex healing process of grafts and bone tunnels after ACL reconstruction. Some studies have verified that DTI can be used to quantitatively evaluate the ACL injury grade and the development of ACL grafts in vivo using a clinical 3.0-Tesla (3.0T) scanner.<sup>14,15</sup> To the best of our knowledge, however, no study has evaluated the fibrous microstructure of the ACL using 7.0T MRI.

Thus, the purpose of this study was to determine the usefulness of 7.0T MRI in assessing the fibrous microstructure of the ACL, specifically by using DTI to reconstruct the three-dimensional (3D) tissue fibre structure in detail.

## Materials and methods

### *Sample collection and preparation*

Eight hind legs from approximately 6-month-old pigs were randomly obtained from the market and evaluated in this study. All samples were fresh pork shanks from pigs that had been slaughtered the same morning. The ACL was extracted with a small amount of bone from the femur and tibia plateau on the attached side of the knee joint (Figure 1). The size of the extracted bone was approximately  $2.5 \times 2.5$  cm. The ligament was approximately 2 cm long and covered a

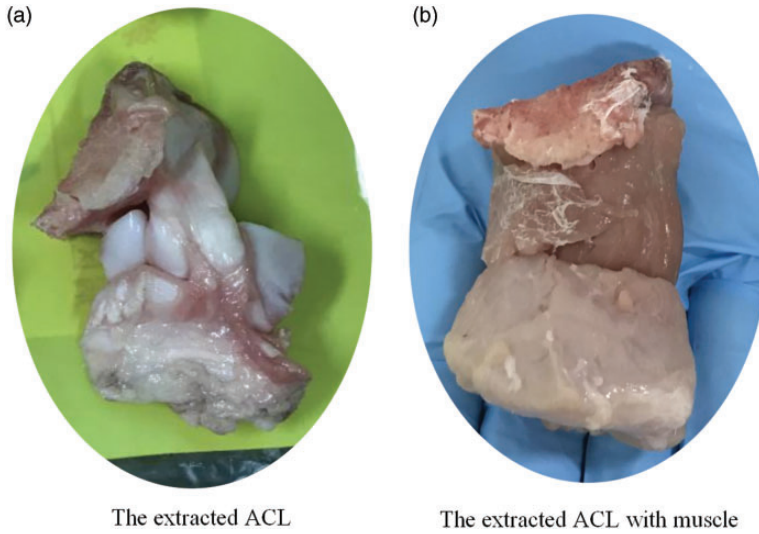


**Figure 1.** (a) Anterior cruciate ligament extracted from the knee joint with little bone from the femur and the tibial plateau on the attached side and (b) The specimen rolled by muscle.

round of pork meat to improve the signal-to-noise ratio (SNR). This study was approved by the ethics review board of Peking University Shenzhen Hospital (approval no. 2019-211-10).

## MRI

MRI scanning was performed with a 7.0T ClinScan (Bruker, Billerica, MA, USA) using a 64-channel knee coil. Imaging experiments were conducted using a 3D localiser (gradient echo) scanner and a standard mouse head coil. The extracted ligament  $\lambda_1$  was positioned at the centre of the coil. A routine diffusion-weighted spin-echo echo-planar imaging pulse sequence was applied to collect a series of axial two-dimensional images of each ligament by using parameters optimised for the skeletal muscle: field of view =  $25 \times 25$  mm,  $b = 600$  s, gradient direction = 20, repetition time = 690 ms, echo time = 15.03 ms, flip angle =  $90^\circ$ , number of excitations = 20, matrix size =  $100 \times 100$ , slice thickness = 1 mm, and zero spacing.

## Data analysis and visualisation

The Diffusion Toolkit on TrackVis software ([www.trackvis.org](http://www.trackvis.org)), written in C++ using the graphical user interface Trolltech Qt 4.2, was used for diffusion tensor MRI analysis and plotting, and Visualization Toolkit 5.0 ([vtk.org](http://vtk.org)) was used to view the images. The singular value decomposition algorithm was used to calculate the eigenvectors of the ACL ( $V_1$ ,  $V_2$ , and  $V_3$ ) and the eigenvalues of the diffusion tensor ( $\lambda_1$ ,  $\lambda_2$ , and  $\lambda_3$ ). The apparent diffusion coefficient (ADC) and fractional anisotropy (FA) of the fibre within each voxel were calculated using the three diffusion eigenvectors. To obtain the mean FA and ADC values, regions of interest were selected using high-resolution T1-weighted images. The ligament was divided into three equal parts: proximal third, intermediate third, and distal third.

Fibre tractography was performed using the TrackVis program developed at Harvard Medical School. In this algorithm, the fibre tracts are reconstructed along the eigenvector corresponding to the preferred

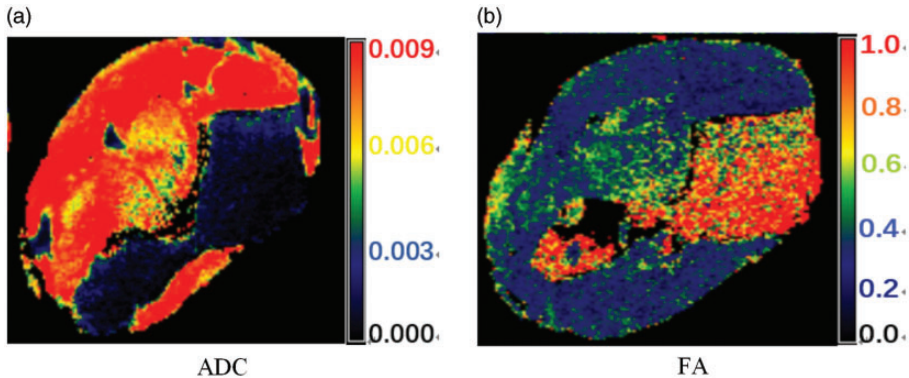


**Figure 2.** The (a) ADC and (b) FA values of one anterior cruciate ligament. In (a), the red portion represents the muscle, the green portion represents ligament, and the black with blue portion indicates bone. ADC, apparent diffusion coefficient; FA, fractional anisotropy.

eigenvalue of the diffusion tensor. The macro-fibre tracts were calculated based on the FA values and the tensor line progressive algorithm of the clip feet near the voxel points. Data were analysed using IBM SPSS Statistics for Windows, Version 19.0 (IBM Corp., Armonk, NY, USA). Continuous variables are expressed as mean  $\pm$  standard deviation, and comparisons among groups were performed using the dependent t test for continuous variables. For all analyses, a *P* value of  $<0.05$  was considered statistically significant.

## Results

The mean FA and ADC for the ACL were  $0.27 \pm 0.079$  and  $0.0012 \pm 0.0005$ , respectively. There were no statistically significant differences between the values in the proximal and distal portions of the ACL. However, the ADC in the centre of the ACL was smaller than those on the sides (mean ADC,  $0.0015 \pm 0.0007$ ;  $P=0.03$ ), and the mean FA in the centre was larger than those on both sides (mean FA,  $0.42 \pm 0.23$ ;  $P=0.01$ ). The FA and ADC maps of a representative ACL were generated and are presented in Figure 2.

The ACL fibre structures of the principal eigenvectors in the background of the DTI scan are shown in Figure 3. The dark grey portion of A represents the ACL. In the fibre tractography analysis of the ACL, this is indicated by a red circle. In this portion, some fibres crossed each other whereas others were parallel to each other. Overall, the fibre shape of the entire ligament was differentiated; some of the fibres were parallel, forming different regions, and the regions intersected one another.

## Discussion

DTI has been used to analyse the brain stem and myocardium, which contain more free hydrogen protons and can show a clearer image in DTI analysis.<sup>11,13</sup> In the present study, several isolated ligaments were imaged using DTI. The most important aspect of this study is that it is the first to obtain images of the fibrous microstructure of the ACL using a DTI sequence with 7.0T MRI. In the 3D figures obtained in this experiment, each fibre showed different colours in the strike direction, and the representative directions were different. The images showed parallel and intersecting fibres in different regions of the same

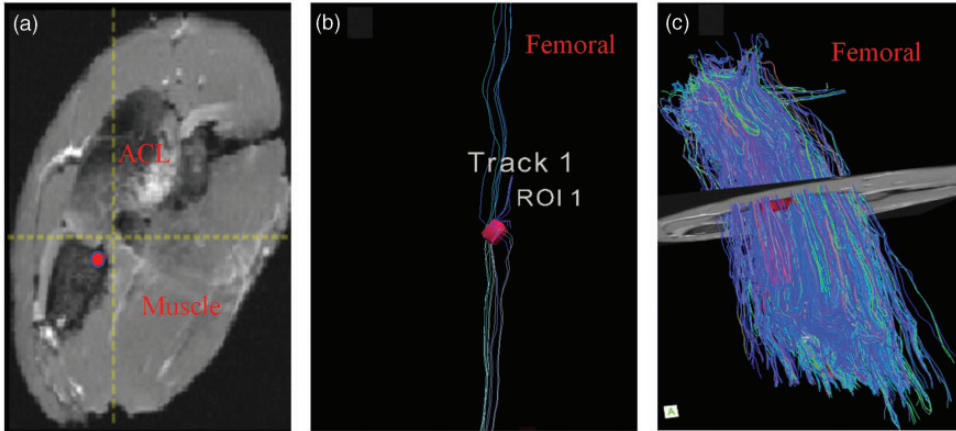


**Figure 3.** Axial images of the ACL with muscle. The images are shown in the following order: (a) high-contrast T1-weighted image obtained using the spoiled gradient recalled pulse sequence, (b) fibre tracking of a small selected portion (red circle in (a)) of the ACL, and (c) fibre tracking of ACL integrity (the fibres were parallel on the proximal and distal sides and were interweaved in the centre). ACL, anterior cruciate ligament; ROI, region of interest.

ACL in each of the eight tested samples. These findings can be attributed to the cell array, which differs with stress and the kinematics of sports.<sup>16</sup> Hatakenaka et al.<sup>17</sup> reported the stress distribution within the ACL body as well as that over the surface, the 3D deformations and stress distributions of the ACL viewed from other sides in addition to those from the medial side, and the variations in the stress distribution pattern in the ACL when the tibia was displaced anteriorly or posteriorly.

In this study, the degree of ACL tissue anisotropy was characterised by the mean FA and ADC. The mean FA tended toward 1, indicating that the structure had a strong degree of anisotropy.<sup>18</sup> The mean FA in the central portion was larger than those in the proximal and distal portions. This indicates that the fibres at the centre of the ACL have a stronger degree of anisotropy due to the interaction of fibres in the middle portion of the ACL. Thus, most of the fibres within the centre are oriented differently, and the collagen fibres are arranged in a disorderly cross pattern. Most of the fibres were

ordered in the same way on both lateral sides. This result is similar to the findings reported in a study in 2013, wherein the FA and ADC values of all portions in the human ACL showed no statistically significant differences.<sup>11,12</sup>

In this experiment, not all ACLs were imaged using DTI. In isolated ligaments, the free water content is further lost, and the resulting imaging data may be influenced by wrapping of the muscle around the ligaments. Because the ACL is composed of dense connective tissue, the number of mobile hydrogen protons in water molecules is low, and the formation of macromolecules results in longer echo times, causing greater attenuation during signal acquisition. Therefore, the SNR is relatively low.<sup>19,20</sup> The diffusion-sensitive factor (b value) represents the degree of sensitivity in diffusional movements. The current range of b values provided by the MRI equipment was 0 to 10000 s/mm<sup>2</sup>. The diffusion sensitivity of water molecules in MRI increases with increasing b-values, but the SNR decreases accordingly. The b value used in this study



was 600 m/s, which was also responsible for the low SNR. The degree of signal reduction depends on the tissue type, tissue structure, physical and physiological states, and microenvironment.<sup>21,22</sup>

This study had some limitations. First, no human ACLs were tested in this study. Therefore, the findings obtained in this study cannot completely represent the data for humans. Human experiments will be conducted in the future. Second, the error in the analysis of the ligaments was very large because the SNR was low. To reduce this error, the voxel size should be increased in future experiments or micro-computed tomography should be used instead to yield a more representative analysis of the ligament fibre structure and obtain more accurate results.

## Conclusions

This study verified the ability to assess the fibrous microstructure of the ACL by 7.0T MRI and yielded the first such images of the ACL fibres. The fibre shape of the ACL was differentiated. The fibres were parallel on the proximal and distal sides; however, they were interweaved in the centre. These imaging results provide a theoretical basis for future development of artificial ACLs in clinical reconstruction.

## Data availability

No data were used to support this study.

## Declaration of conflicting interest


The authors declare that there is no conflict of interest.

## Funding

The authors disclosed receipt of the following financial support for the research, authorship, and/or publication of this article: This work was partially supported by the clinical research project of Peking University Shenzhen Hospital (No. LCYJ2020005), the Medical Scientific

Research Foundation of Guangdong Province (Nos. A2017202 and A2016517), the Natural Science Foundation of Guangdong Province (No. 2017A030310616), and Guangdong Sports Bureau (No. GDSS2020N002).

## ORCID iD

Tian You  <https://orcid.org/0000-0001-7027-7230>

## References

1. Florisson JMG, Dudink J, Koning IV, et al. Assessment of white matter microstructural integrity in children with syndromic cranio-synostosis: a diffusion-tensor imaging study. *Radiology* 2011; 261: 534–541.
2. Zijta FM, Lakeman MME, Froeling M, et al. Evaluation of the female pelvic floor in pelvic organ prolapse using 3.0-Tesla diffusion tensor imaging and fibre tractography. *Eur Radiol* 2012; 22: 2806–2813.
3. McCauley TR, Moses M, Kier R, et al. MR diagnosis of tears of anterior cruciate ligament of the knee: importance of ancillary findings. *AJR Am J Roentgenol* 1994; 162: 115–119.
4. Pietsch M and Hofmann S. Value of radiographic examination of the knee joint for the orthopedic surgeon. *Radiologe* 2006; 46: 55–64.
5. Le Bihan D, Mangin JF, Poupon C, et al. Diffusion tensor imaging: concepts and applications. *J Magn Reson Imaging* 2001; 13: 534–546.
6. Motyka S, Moser P, Hingerl L, et al. The influence of spatial resolution on the spectral quality and quantification accuracy of whole-brain MRSI at 1.5T, 3T, 7T, and 9.4T. *Magn Reson Med* 2019; 82: 551–565.
7. Choi SJ, Lim KO, Monteiro I, et al. Diffusion tensor imaging of frontal white matter microstructure in early Alzheimer's disease: a preliminary study. *J Geriatr Psychiatry Neurol* 2005; 18: 12–19.
8. Parker GJM. Analysis of MR diffusion weighted images. *Br J Radiol* 2004; 77: S176–S185.
9. Rousset P, Delmas V, Buy JN, et al. In vivo visualization of the levator ani muscle subdivisions using MR fiber tractography with

- diffusion tensor imaging. *J Anat* 2012; 221: 221–228.
10. Zaraiskaya T, Kumbhare D and Noseworthy MD. Diffusion tensor imaging in evaluation of human skeletal muscle injury. *J Magn Reson Imaging* 2006; 24: 402–408.
  11. Wengler K, Tank D, Fukuda T, et al. Diffusion tensor imaging of human Achilles tendon by stimulated echo readout-segmented EPI (ste-RS-EPI). *Magn Reson Med* 2018; 80: 2464–2474.
  12. Chen L, Zhao H, Li J, et al. Diffusion tensor imaging map of anterior cruciate ligament contrasted with MRI in healthy adults. *Zhong Nan Da Xue Xue Bao Yi Xue Ban* 2013; 38: 610–616.
  13. Delin C, Silvera S, Coste J, et al. Reliability and diagnostic accuracy of qualitative evaluation of diffusion-weighted MRI combined with conventional MRI in differentiating between complete and partial anterior cruciate ligament tears. *Eur Radiol* 2013; 23: 845–854.
  14. Dyck PV, Billiet T, Heusdens C, et al. Diffusion tensor imaging of the anterior cruciate ligament graft following reconstruction: a longitudinal study. *Eur Radiol* 2020; 30: 6673–6684.
  15. Liu S, Liu J, Chen W, et al. Diffusion tensor imaging for quantitative assessment of anterior cruciate ligament injury grades and graft. *J Magn Reson Imaging* 2020; 52: 1475–1484.
  16. Sinha U, Sinha S, Hodgson JA, et al. Human soleus muscle architecture at different ankle joint angles from magnetic resonance diffusion tensor imaging. *J Appl Physiol (1985)* 2011; 110: 807–819.
  17. Hatakenaka M, Yabuuchi H, Sunami S, et al. Joint position affects muscle proton diffusion: evaluation with a 3-T MR system. *AJR Am J Roentgenol* 2010; 194: W208–W211.
  18. Basser PJ, Mattiello J, Turner R, et al. Diffusion tensor echo-planar imaging of human brain. In: *Proceedings of the international society for magnetic resonance in medicine*, 1993, pp.584. New York: Wiley.
  19. Cheryauka AB, Lee JN, Samsonov AA, et al. MRI diffusion tensor reconstruction with PROPELLER data acquisition. *Magn Reson Imaging* 2004; 22: 139–148.
  20. Forbes KP, Pipe JG, Karis JP, et al. Improved image quality and detection of acute cerebral infarction with PROPELLER diffusion-weighted MR imaging. *Radiology* 2002; 225: 551–555.
  21. Busch E, Hoehn-Berlage M, Eis M, et al. Simultaneous recording of EEG, DC potential and diffusion-weighted NMR imaging during potassium induced cortical spreading depression in rats. *NMR Biomed* 1995; 8: 59–64.
  22. Hasegawa Y, Latour LL, Formato JE, et al. Spreading waves of a reduced diffusion coefficient of water in normal and ischemic rat brain. *J Cereb Blood Flow Metab* 1995; 15: 179–187.